Hydrology Research

Hydrology Research Vol 55 No 6, 595 doi: 10.2166/nh.2024.192

The phenomenon of drought in Ethiopia: Historical evolution and climatic forcing

Getachew Mehabie Mulualem [a,*], U. Jaya Parakash Raju[b], Milica Stojanovic[c] and Rogert Sorí[c]

[a] Department of Mathematics, College of Science, Bahir Dar University, P.O. Box 79, Bahir Dar, Ethiopia
[b] Department of Physics, College of Science, Bahir Dar University, P. O. Box 79, Bahir Dar, Ethiopia
[c] Centro de Investigación Mariña, Universidade de Vigo, Environmental Physics Laboratory (EPhysLab), Campus As Lagoas s/n, Ourense 32004, Spain
*Corresponding author. E-mail: getch@aims.ac.za

GMM, 0000-0002-6488-4402

ABSTRACT

This study examines drought patterns in Ethiopia's 12 major river basins from 1981 to 2018 using the Standardized Precipitation Index (SPI) and the Standardized Precipitation Evapotranspiration Index (SPEI). Both indices reveal historical drought episodes with slight variations, with significant differences in 1984, 2009, and 2015. Except for the Wabi-Shebelle catchment in southern Ethiopia, all river basins show an increasing trend in SPI12 and SPEI12 indices. The eastern and central regions experience more drought according to SPEI3. Seasonal correlations show that during the March–May rainy season, precipitation is negatively correlated with the Indian Ocean Dipole (IOD) index, while in the June–September season, it negatively correlates with Nino 3.4 and positively with IOD. The study also found that El Niño leads to less rainfall in the Ethiopian highlands, while La Niña results in more rainfall in the central and northern highlands but less in the south.

Key words: droughts, Ethiopian basins, SPI and SPEI, teleconnections

HIGHLIGHTS

- The research assessed Ethiopia's drought conditions and their environmental implications using the SPI and SPEI, identifying significant drought periods in 1982, 1984, 1987, 1991, 1997, 2002, 2006, 2011, and 2015, with both indices showing a similar drought progression but with slight differences in severity.
- The research revealed that the discrepancy between the SPI and SPEI is consistently negative. This underscores the crucial influence of temperature and evapotranspiration processes in assessing the severity of droughts.
- The research evaluated the impact of multiple teleconnections on drought conditions. It was observed that distinct precipitation anomaly patterns across Ethiopia were linked to variations in Sea Surface Temperature (SST).
- The results highlight the relationship of El Niño with the occurrence of drought conditions in Ethiopia, particularly its effect on cumulative drought conditions for time scales of more than 6 to 12 months. The effects of the La Niña event on drought conditions in Ethiopia are not clearly observed, as several areas experienced abnormally wet conditions during La Niña events.

GRAPHICAL ABSTRACT

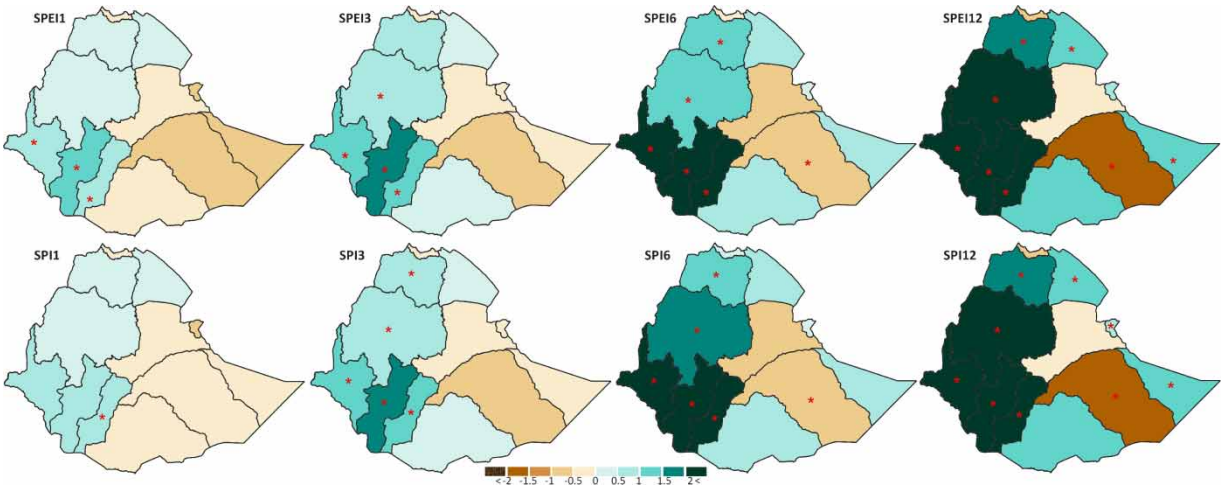

INTRODUCTION

Drought is a dry period in the climate system caused by the lack of rainfall, that can occur anywhere in the world. It is a slow-onset disaster characterized by the lack of precipitation, resulting in a water shortage. Hence, its frequency and severity can produce devastating effects on agriculture, the environment, the economy, energy, and also human health (Naumann *et al.* 2021; Salvador *et al.* 2023). Unfortunately, drought has become a more recurring phenomenon in many countries of the world due to global warming, climate change, and direct human activities (IPCC 2021; Li *et al.* 2021). Sub-Saharan Africa is one of the driest regions in the world, and even recent findings from the Intergovernmental Panel on Climate Change (IPCC) (Trisos *et al.* 2022) provide ample evidence that climate change is affecting large parts of this region. Ethiopia is one of the sub-Saharan countries that has experienced many severe droughts in its history of the past six decades (a total of 30 drought events, 13 of which were severe and affected the entire country), seriously affecting a population of millions of people (Zeleza & McCann 1997; Gebrehiwot *et al.* 2011; Bayissa *et al.* 2015). Currently, the occurrence of drought in the country is increasing rapidly (once every 2–3 years) compared to the recent past (once every 10 years) (Gebrehiwot *et al.* 2011; Zinna & Suryabhagavan 2016). This represents a high risk, as the economy of Ethiopia is largely dependent on rain-fed agriculture, which accounts for approximately 49% of the country's GDP, with more than 80 million people dependent on agriculture (Silva & Uchida 2000, CSA 2014). Even small changes in rainfall patterns directly affect the agricultural sector, damaging crops and reducing yields. In a worst-case scenario, this could lead to a famine that kills more than a million people. The drought of 1984–1985 is still fresh in the memories of many Ethiopians, as it claimed the lives of more than 200,000 people and damaged millions of livestock (Kumar 2008).

According to the scientific literature, drought is categorized into meteorological, agricultural, hydrological, and socio-economic droughts (Tallaksen & Van Lanen 2004; Zhong *et al.* 2019), developing slowly over time and space (Lehner *et al.* 2001). Hence, the development of trustworthy and measurable drought indices is vital for drought monitoring and characterization (Zargar *et al.* 2011). By applying diverse drought indices according to their suitability for drought analysis at different timescales, it can be applied to drought monitoring. For example, the Standardized Precipitation Index (SPI) is widely used to monitor droughts as it is recommended for this purpose by the World Meteorological Organization (WMO). Its multivariate character allows for evaluating dry/wet conditions at various accumulation periods of anomalous precipitation, which can be associated with different drought types, such as SPI-1 for meteorological drought, SPI3–SPI6 for agricultural drought, and SPI6–SPI24 for hydrological drought (Tsakiris *et al.* 2007; Kaniewski *et al.* 2012, WMO 2012; Adnan *et al.* 2015, 2018; Tigkas *et al.* 2015; Mondol *et al.* 2016). Many drought indices have been utilized to quantify and characterize drought events, but each has its strengths and weaknesses (Park *et al.* 2014; Jain *et al.* 2015). In developing countries such as Ethiopia, precipitation is readily available only through ground-based rain gauges, so several previous studies in Ethiopia point out that the SPI index can be utilized to assess drought. For instance, Bayissa *et al.* (2015, 2018) used SPI for the assessment of drought conditions in the Upper Blue Nile (UBN) region, Suryabhagavan (2017) for various regions of Ethiopia,

Gebrehiwot *et al.* (2011) for drought in the highlands of northern Ethiopia, Edossa *et al.* (2010) for Awash River Basin, and Gidey *et al.* (2018) for Raya Basin.

One of the weaknesses of SPI is to measure dryness in desert areas where evaporation is an important source of moisture (Almedeij 2014). Thus, the developed Standardized Precipitation Evapotranspiration Index (SPEI) tracks a similar approach to SPI, but it is based on a monthly climatic water balance, taking into account the role of temperature, which is the crucial strength of the SPEI over the broadly utilized drought indices (Vicente-Serrano *et al*. 2010; Yu *et al.* 2014). Recently, Mulualem & Liou (2020) predict the SPEI index in the UBN basin using an artificial neural network model incorporating multiple variables such as hydro-meteorological, climate, sea surface temperature (SST), and topographic features from 30 years of time series data. They found that the model shows a great level of similarity among observed and predicted SPEI values. The study conducted by Kourouma *et al.* (2022) investigated spatiotemporal climate variability of drought characteristics in 16 localities of Ethiopia in the period 1983–2020 using SPI and SPEI indices at different timescales. They concluded that the frequency, magnitude, and severity change spatially by area and the longest drought persisted for 12 months in the year 2015. Lemma *et al.* (2022) assessed meteorological drought in selected Ethiopian watersheds (Awash, UBN, Baro, Danakil, Omo, and Tekeze) using the Climate Hazard Group Infrared Precipitation Station (CHIRPS) dataset to calculate SPI and Effective Drought Index (EDI), confirming the usefulness of these data for this purpose. In a recent study, Stojanovic *et al.* (2022) also investigated the period 1980–2018 characterized by extreme drought conditions in hydro-climatological regions of Ethiopia and the role of moisture transport to precipitation from climatological sources.

The variability of drought events in Ethiopia has been hypothesized to be related to the anomaly of ocean circulations through atmospheric circulations. For example, the El Niño-Southern Oscillation (ENSO) phenomenon greatly affects Ethiopian precipitation (Camberlin 1997). The connection between El Niño events and drought in Ethiopia has been comprehensively reviewed by many researchers using a long historical rainfall record (Wolde-Georgis 1997; Comenetz & Caviedes 2002; Roop *et al.* 2016; Ahmed *et al.* 2017; Mersha & van Laerhoven 2018). A list of El Niño and La Niña events and affected regions in Ethiopia is presented in Table 1. Comenetz (2002) investigated the correspondence of the warm phase of ENSO cycles to drought events in Ethiopia, revealing that the 1997/98 El Niño caused a very abnormal rainfall distribution and the consequences were reduced crop production, outbreaks of cholera and cerebral malaria, deaths, and property damage (Babu 2009). Koo *et al.* (2019) divided ENSO events in Ethiopia into three periods: 2015/2016 El Niño, 2016/2017 La Niña, and neutral years (i.e. 2012/2013, 2013/2014, 2014/2015, and 2017/2018), to examine crop yield effects of climate change linked with ENSO phases at each grid element of agro-ecological zone level and revealed that the combination of El Niño and La Niña determines the final agricultural yields in Ethiopia. Some authors study ENSO effects on river basins in Ethiopia (Attia & Abulhoda 1992; Eltahir 1996; Molla *et al.* 2019). Some authors examine the effects of ENSO on Ethiopian river basins, showing that ENSO episodes are negatively correlated to the floods of the Blue Nile and Atbara rivers originating in Ethiopia and affecting the Nile River flow (which is the source of 85% of the Nile water) (Attia & Abulhoda 1992; Eltahir 1996; Molla *et al.* 2019).

Table 1 | Timeline of ENSO years and droughts in Ethiopia

ENSO years	Droughts	Affected regions
1982–1983	1983–1984	All regions, particularly Tigray and Wollo
1986–1987	1987–1988	All regions
1991–1992	1990–1992	North, East, and South Ethiopia
1993	1993–1994	Tigray and Wollo
2000	2000	All regions
2002–2003	2002–2003	North, East, and Central Ethiopia
2008–2009	2006	The Southern Nations, Nationalities, and Peoples' Region (SNNPR) (Borena)
2009–2010	2008–2009	North, East, Central, and South Ethiopia
2011	2010–2011	South-central, Southeastern, and Eastern parts of Ethiopia
2015–2016	2015–2016	Oromia, Somali, Amhara, Afar, Tigray, SNNPR

Although several previous studies have evaluated drought in Ethiopia, the spatial and temporal variability of drought has not been established, particularly at the local and sub-regional levels. This is important because many drought studies emphasize short-term analysis (Bewket & Conway 2007), specific season analysis (Viste *et al.* 2013), or study the drought conditions in certain regions rather than the whole country (Bewket & Conway 2007; Edossa *et al.* 2010).

In this paper, we address a significant gap in the understanding of historical droughts in Ethiopia's 12 large river basins. Despite numerous studies on the impact of drought during Ethiopia's historical period and the drought situation in Ethiopia, there is a lack of comprehensive spatial and temporal estimates of these droughts. Our research fills this gap by using 38 years of meteorological variables (precipitation and temperature) to estimate these droughts.

We also extend the existing body of knowledge by studying the regional distribution of meteorological and hydrological drought. We calculate SPI and SPEI at 1–12 timescales and calculate long-term trends using the Mann–Kendall (M–K) test in all catchment areas. This analysis allows us to examine the frequency of drought events at regional and sub-regional scales and its relationship with oceanic impact (Dipole Mode Index (DMI), Oceanic Niño Index (ONI), Pacific Decadal Oscillation (PDO), and Southern Oscillation Index (SOI)) seasonally in all water bodies using the CHIRPS precipitation dataset. Furthermore, we address another research gap regarding the unclear relationship between the ENSO occurrence and its effects on different parts of the country (AKLDP 2015). Our research, focused on major river basins in Ethiopia, provides important insights to manage agricultural systems, plan water resources, and adapt ecological systems to future climate change. It also helps predict drought events and its critical parameters to improve early warning capabilities for drought management. We believe that our approach, while challenging, can significantly contribute to drought management by targeting the most vulnerable areas.

STUDY AREA AND DATA

Study area

Ethiopia consists of a vast highland complex of mountains, plateaus, and lakes and is situated in the east part of Africa (Figure 1). Due to the complex topographical and geographical features, the climate of Ethiopia shows considerable spatial variation and different precipitation regimes (Zeleke *et al.* 2013). According to elevation, three climatic regions are recognized, namely, the tropical (1,830 m) with an average annual temperature of 20–28 °C, the subtropical zone (1,830–2,440 m) with an average annual temperature of 16–20 °C, and a cold zone (above 2,440 m) with an average annual temperature between 6 and 16 °C (Viste *et al.* 2013).

Ethiopia comprises 12 major rivers, and 5 of them are transboundary rivers. The river basins are considered hydrological units defined orographically to a large extent by historical precipitation, which ultimately contributes to the volume of groundwater and river systems. The Blue Nile is the largest river in Ethiopia, which originated from Lake Tana in the northwestern part of the highlands. Next, it flows through Sudan, where, in the area of Khartoum, it joins with the White Nile (Billi 2015). The other rivers flow to the Mediterranean Sea, the Indian Ocean, or into the Endorheic basins. Because of

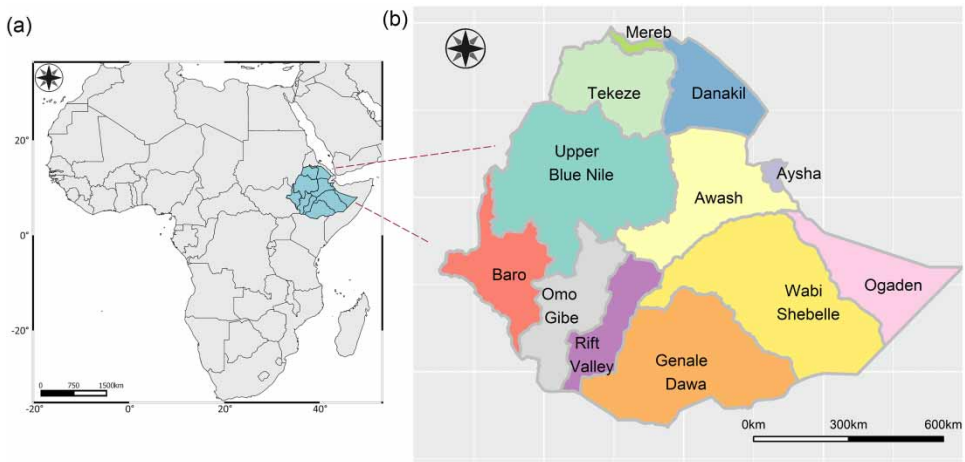

Figure 1 | The geographical location of Ethiopia (a) and schematic representation of the main river basins (b).

its out-flowing rivers to the neighboring countries, Ethiopia is commonly referred to as a water tower in East Africa. The 12 river basins (Figure 1) have an estimated total flow of 122 billion metric cubes and an estimated 2.6–6.5 billion metric cubes of groundwater potential (Awulachew *et al.* 2007). Out of these major basins, Aysha, Danakil, Ogaden, and Mereb river basins contain no continuously flowing rivers (Ambelu 2009). Ethiopia has three drainage systems. The Western is the largest one constituting the Tekeze, Blue Nile (also called Abbay Basin), and Baro and flows into South Sudan and Sudan. The second one is the Rift Valley comprising the Awash and Omo Rivers. Omo flows into Lake Turkana on the border of Kenya. In contrast, Awash flows northeast of the Danakil depression and then dissipates into a chain of swamps and lakes at the border of Djibouti. The third consists of the rivers Shebelle and Genale originating from the mountains of the east and flowing into Somalia and the Indian Ocean.

METHODOLOGY AND DATASETS

Datasets

The precipitation data from the CHIRPS (v2.0) (Funk *et al.* 2015) for the 1981–2018 period was utilized for the computation of drought indices. CHIRPS is a 30+ year quasi-global precipitation dataset linking satellite observations from the National Climate Forecast System version 2 and *in situ* precipitation observations (Dai 2013). This dataset combines satellite products and ground stations to form a gridded precipitation time series and is available at an original spatial resolution of 0.05° with a global coverage ranging from 50°S to 50°N. This dataset has been widely used for monitoring the precipitation variability and drought conditions in Ethiopia (Belay *et al.* 2019). Among the presently accessible satellite rainfall products, CHIRPS has better performance and is therefore suggested as a valuable substitute for the gauge precipitation dataset (Gebremedhin *et al.* 2021). A recent public study by Ahmed *et al.* (2024) evaluated the performance of ERA5 reanalysis data and CHIRPS precipitation data against ground-based measurements from 167 rain gauges in Ethiopia. These authors used point to pixel analysis for the period 1980–2018 to compare daily, monthly, seasonal, and annual precipitation data. The result indicated that over Ethiopia, CHIRPS generally outperforms ERA5, particularly in high-altitude areas, demonstrating a better capability in detecting high-intensity precipitation events. They also highlight considerable performance differences between CHIRPS and ERA5 across varying Ethiopian landscapes and climatic conditions. CHIRPS effectiveness in high-altitude regions, especially for daily precipitation estimation, emphasizes its suitability in similar geographic contexts. It has also been confirmed that CHIRPS can supplement the sparse rain gauge network and afford high spatial and temporal resolution for trend analysis (Dinku *et al.* 2007; Hirpa *et al.* 2010; Ayehu *et al.* 2018; Fenta *et al.* 2018). The CHIRPS data are downloaded from the FTP server (ftp://ftp.chg.ucsb.edu/pub/org/chg/products/CHIRPS-2.0).

The ONI and the Indian Ocean Dipole (IOD) are utilized to see how rainfall responds to climatic conditions. The National Oceanic and Atmospheric Administration's (NOAA) operational definitions of El Niño and La Niña conditions are based on the ONI. The ONI tracks the running 3-month average SST in the east-central tropical Pacific near the International Dateline, and whether they are warmer or cooler than average. The ONI is defined as the 3-month running means of SST anomalies in the Niño 3.4 region (5°N–5°S, 120°W°–170°W). The 3-month average temperature anomaly time series was retrieved from the NOAA website (https://www.cpc.ncep.noaa.gov/data/indices/oni). However, the IOD is obtained by taking the differences among the SST anomalies in the western (50°E–70°E, 10°S–10°N) and eastern (90°E–110°E, 10°S–0°N) portions of the Indian Ocean (Saji *et al.* 1999). The monthly IOD data are downloaded from http://www.jamstec.go.jp/frcgc/research/d1/iod/iod/dipole_mode_index.html. Furthermore, the PDO is commonly described as a long-lasting El Niño-like pattern of Pacific climate fluctuation. The PDO index values used here are from NOAA's Earth System Research Laboratory (ESRL) (http://www.esrl.noaa.gov/psd/data/correlation/pdo.data), which provides data from 1948 to the present.

Methodology

The SPI and SPEI

The SPI is the most commonly used indicator worldwide designed by McKee *et al.* (1993) for identifying meteorological droughts. The SPI calculates precipitation anomalies at a given position based on a comparison of observed precipitation amounts for the period of interest (e.g. 3, 6, 12, 24 months) with the long-term historical precipitation record for that period. In general, the historical record is fitted to a Gamma probability distribution, which is then back-transformed to a normal distribution such that the mean of the SPI values becomes zero and the variance of one. Conceptually, SPI is equivalent to the *Z*-score, which is a commonly used technique in statistics. Detailed formulation and more information on the SPI can be found in Mckee *et al.* (1993) and WMO (2012). We have to take into consideration that the SPI shows the anomalies of the

observed total precipitation for any given location and accumulation period of interest. Thus, the magnitude of the departure from the average value is a probabilistic measure of the severity of wet (positive values) or dry (negative values) conditions. Since SPI can be calculated over different precipitation accumulation periods (typically ranging from 1 to 24 months), the resulting various SPI indicators allow for estimating different potential impacts of drought. In conventional and operational applications, SPI1–SPI3 indicate immediate consequences such as reduced soil moisture, snowpack, and flow in smaller creeks; SPI3–SPI12 are used as indicators for reduced stream flow and reservoir storage, while SPI12–SPI24 are used as indicators for reduced reservoir and groundwater recharge. To get a full picture of the potential impacts of drought, the SPI should be calculated and compared at different timescales, and also a comparison with other drought indicators is also needed. One of the disadvantages of SPI is that it takes into account only precipitation and can fail to measure the role of temperature and other meteorological variables like the wind on the evaporation from the surface and, therefore, their role in the occurrence and severity of drought (Vicente-Serrano *et al.* 2010). For this reason, the SPEI is also used in this study.

The SPEI utilized the same method as the SPI, but its sensitivity to evapotranspiration permitted it to assess the water supply and demand relationships at various timescales (Yu *et al.* 2014). Its multi-scalar characteristics also permit the assessment of the temporal evolution of the climatic water balance, which facilitates the attribution of drought occurrence and severity at different timescales (Beguería *et al.* 2010). Thus, potential evapotranspiration (PET) is a crucial water loss indicator to consider for investigating drought conditions in the hydrological cycle in the context of global warming (Mukherjee *et al.* 2018). Vicente-Serrano *et al.* (2010) described the method to calculate the SPEI, which takes as input data the difference between precipitation and PET. For calculating PET, there are various methodologies, such as the Thornthwaite (Thornthwaite 1948), the Hargreaves (Hargreaves 1975), the modified Hargreaves (Ravazzani *et al.* 2012), and the Penman–Monteith FAO56 methods (Allen *et al.* 2006). Based on SPI/SPEI indices, a classification of drought into seven categories ranging from an extremely dry to an extremely wet class is given in Table 2. A drought episode starts when the SPI/SPEI value is below zero, followed by a value of −1 or less, and ends when the SPI/SPEI returns to a positive value (Mckee *et al.* 1993). The severity of each episode is calculated by summing all SPI/SPEI values over the months of the episode.

M–K trend test

The M–K trend test (Mann 1945) is a non-parametric method widely used to detect significant trends in time series data. It identifies the presence of a monotonic tendency in a chronological series of a variable, with the null hypothesis stating that there is no monotonic trend. The test does not make assumptions about the underlying distribution of the data, and its rank-based measure is not influenced by extreme values. The primary output of this method is the Kendall Tau, which measures the monotonicity of the slope. In addition, it provides the Sen's slope, estimating the overall slope of the time series. This makes the M–K trend test a reliable and robust tool for time series analysis. In this study, statistical significance trend analysis was done by using the M–K trend test, while the magnitude of trend was determined by the non-parametric Sen's slope estimator.

RESULTS AND DISCUSSION

Drought episode frequency based on SPI and SPEI

We run a comparative analysis between SPI and SPEI at 1, 3, 6, and 12 temporal scales for the entire country, which represent the multi-temporal nature of drought and its evolution through time (Figure 2). As can be seen in Figure 2, at short

Table 2 | Drought category based on SPI/SPEI values (Mckee *et al.* 1993)

SPI/SPEI values	Drought category
$SPI/SPEI \geq 2$	Extremely wet
$1.5 \leq SPI/SPEI \leq 2$	Severely wet
$1 \leq SPI/SPEI \leq 1.5$	Moderately wet
$-1 \leq SPI/SPEI \leq 1$	Near normal
$-1.5 \leq SPI/SPEI \leq -1$	Moderately dry
$-2 \leq SPI/SPEI \leq -1.5$	Severely dry
$SPEI < -2$	Extremely dry

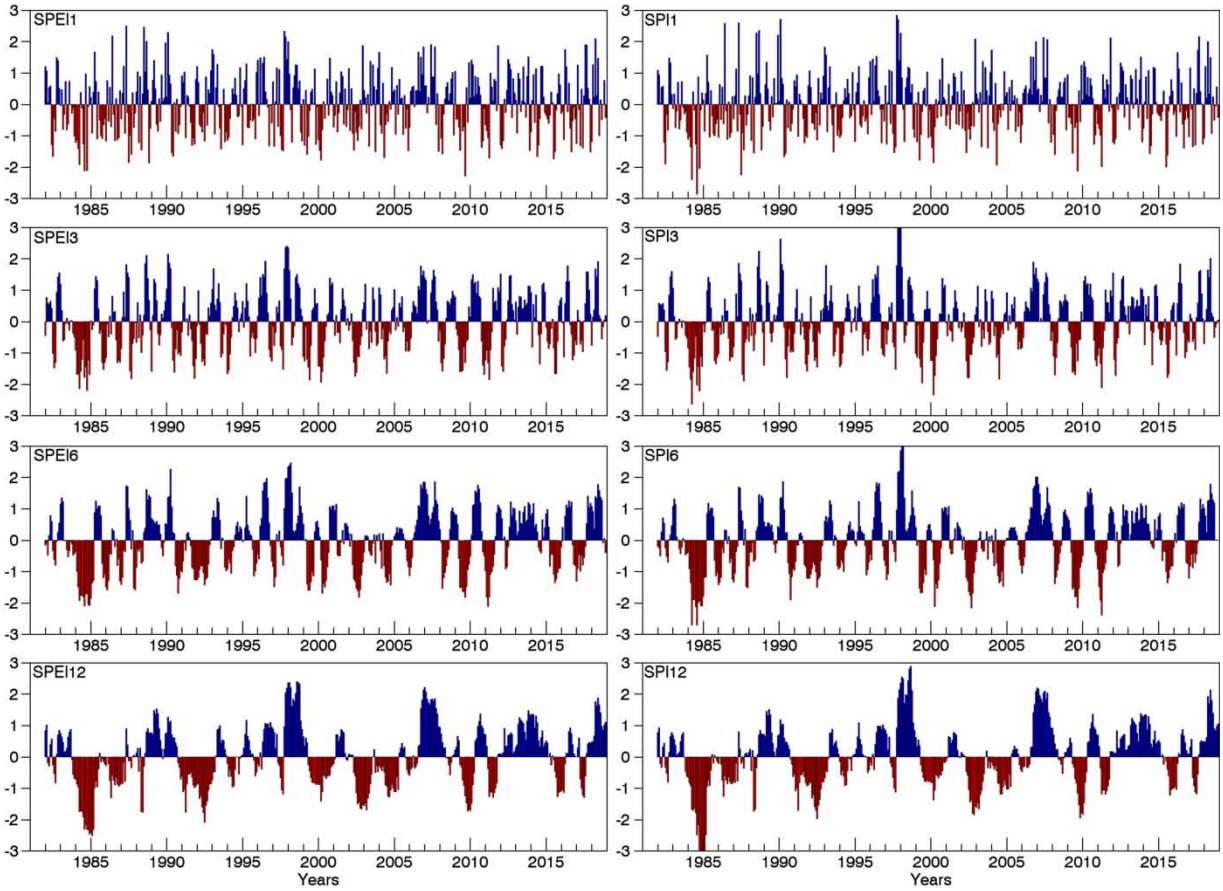

Figure 2 | Temporal evolution of SPI and SPEI over 1-, 3-, 6-, and 12-month timescales for the whole of Ethiopia. Yellow, red, and violet colors represent different drought categorizations.

temporal scales, the variability is greater, so a higher number of flash droughts are normal. The evolution of each series of the SPI1 and SPEI1, SPI3 and SPE3, SPI6 and SPEI6, and SPI12 and SPEI12, reveal a great resemblance between each pair of series, and different drought events can be distinguished below the threshold of −1. A visual analysis of Figure 2 reveals periods of drought that, as the timescale of the indices increases, the duration of dry conditions increases, because the variability of the series is reduced as the hydrological processes that take place seasonally and interannually have less variability. In addition, historical droughts the country faced in the past four decades such as 1984, 2002, 2009, 2011, and 2015 are appreciated at various temporal scales of both the SPI and the SPEI. Stojanovic *et al.* (2022) utilized other precipitation and evapotranspiration datasets (CRU TS v4.05) and also found the affectation of extreme dry conditions in the northeast, southeast, and southwest of the country during 1984, which was associated with a reduction of moisture transport from oceanic and terrestrial sources and divergence of the moisture flux. They also found the affectation of the northeast and west major river basins in 2009.

To better illustrate the evolution of dry conditions and their temporal propagation, we depict in Figure 3 the temporal evolution of dry and wet conditions for Ethiopia through the SPEI and SPI at a temporal scale of 1–12 months. As observed, the SPI and SPEI generally coincide in the identification of drought conditions that propagate over various timescales. The spread from meteorological to hydrological drought is notable for its severity in 1984, as well as other documented affected years such as 1987/1988, 1992/1993, 1999, 2003/2004, 2007/2008, 2011, and 2015. These years have been among the worst drought episode frequency that the country faced in the last century, and similar findings were reported by Gebrehiwot *et al.* (2011), Viste *et al.* (2013), and Bayissa *et al.* (2017). Despite the similarity observed between the indices, the temporal drought analysis results indicate that there is a small difference in magnitude among the droughts described by the precipitation-based SPI, and the temperature influenced SPEI. It can be observed during drought in 2002 and 2004.

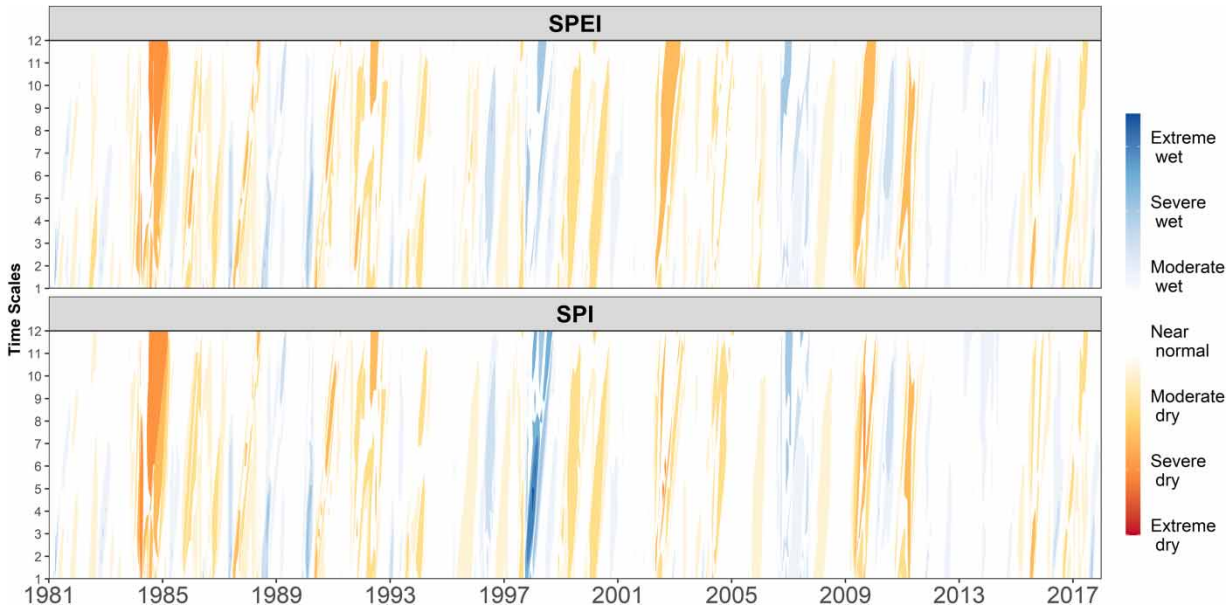

Figure 3 | Temporal evolution of the SPEI and SPI values on different timescales (1–12 months) for the 1981–2018 period for the whole of Ethiopia.

According to Abera & Gebeyehu (2022), previous studies have primarily focused on meteorological drought rather than hydrological and agricultural drought in Ethiopia. Therefore, in this figure, both drought indices are plotted for each basin from 1 to 12 timescales. The analysis of the evolution of dry conditions for each basin is shown in Figure 4. It can be seen that all the basins were affected by severe and extreme drought conditions during 1983 and 1984. The identification of these conditions according to SPI values coincides with the temporal identification of SPI, although in some periods differences in the magnitude of severity are observed. For example, in 1993, the Baro basin, located in the far west of Ethiopia, was affected by extremely dry conditions according to SPEI and SPI values on timescales of 1–12 months, while in the rest of the basins, dry conditions did not reach the same severity during this year. This is also observed for other basins such as the Rift Valley during 1998 and 1999, when it was affected by extreme drought conditions, but basins to the north and south of it were

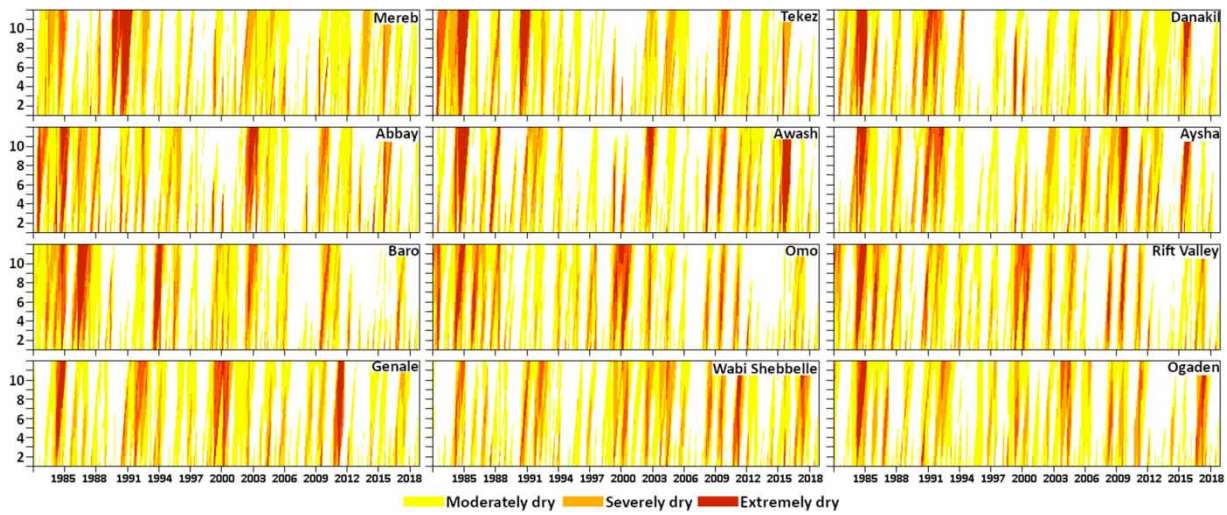

Figure 4 | Temporal evolution of the SPEI and SPI (Supplementary Material Figure S1) values on different timescales (1–12 months) for the 1981–2018 period for each river basin.

affected by dry conditions of lesser magnitude. Differences in drought severity and drought affliction periods are also observed between basins with similar rainfall regimes such as the Abbay and Baro, or Genale, Wabi-Shebelle, and Ogaden (Stojanovic *et al.* 2022). These results suggest that despite the homogeneity in rainfall regimes among some of the major basins in Ethiopia, drought phenomena differ in frequency and severity when basins are considered individually. These differences have also been reported in previous results of Lemma *et al.* (2022), who analyzed basin-wide meteorological droughts for Ethiopia during the 1982–2016 period through the SPI and the EDI using satellite origin rainfall. According to these authors, in almost all river basins, both indices detected maximum severity during 1984/85, 1991/92, 2003, 2013, and 2014, in agreement with other studies. However, our results do not show that the years 2013 and 2014 were severely or extremely dry in any basin.

Drought episode frequency

To provide a more detailed analysis at the hydro-climatic scale, we calculated the frequency of drought events resulting from the two indices in the most representative river basins of Ethiopia. Hence, the drought episode frequency at the 3-month timescale is plotted in Figure 5. The SPEI3 drought frequency revealed higher variability with a higher number of drought episode frequency. Danakil, Awash, Wabi-Shebelle, and Ogden were affected by metrological drought episode frequency. However, SPI3 showed a relatively small frequency of droughts and a similar frequency pattern. Based on the SPEI, more frequent drought episodes were perceived in the eastern parts of the study area than in the central highlands.

The SPEI is chosen for further analysis as it accounts for both the effect of precipitation and temperature in its development. Especially the timescales of SPEI3 and SPEI12 months are investigated for the main basins of the country. In Figure 6, the monthly drought episode frequency for each of the 12 main basins in the period 1981–2018 for SPEI3 and SPEI12 are shown. In January, the highest number of drought episode frequency according to the SPEI3 affected the Rift Valley areas of the country, namely, the Awash and Rift Valley basins (Figure 6(a)). In February, the same situation repeated, but it also included the eastern lowland, the Wabi-Shebelle and Baro basins. In March, the frequency pattern does not change a lot from the February conditions; instead, a more similar frequency pattern was seen this month. In April, the Danakil and Awash basins were hit by a greater number of droughts. The conditions in May and June show the same pattern with high drought episode frequency observed in the basins located in the central and southern regions of the country, namely, Abbay, Awash, Baro, Omo, Gibe, Rift Valley, and Genale. Interestingly, from July to September, the drought episode frequency shifted locations, and a large number of drought episodes affected the Abbay, Awash, Tekeze, Baro, and Rift Valley basins. In October, all basins located in the south of the country had observed a large number of drought episodes. In November, the frequency of drought episodes was greater in Wabi-Shebelle, Genale, and Ogaden basins. Finally, in December, compared to other months, a similar frequency pattern was seen in the whole of the country.

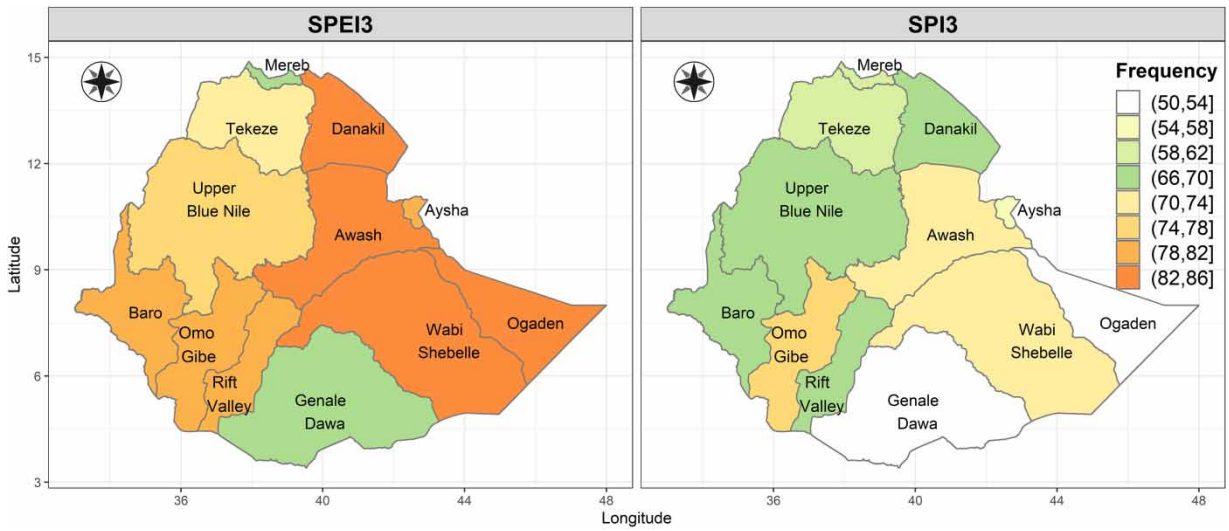

Figure 5 | Annual frequency of drought based on the SPI3 and SPEI3 counts for the period 1981–2018.

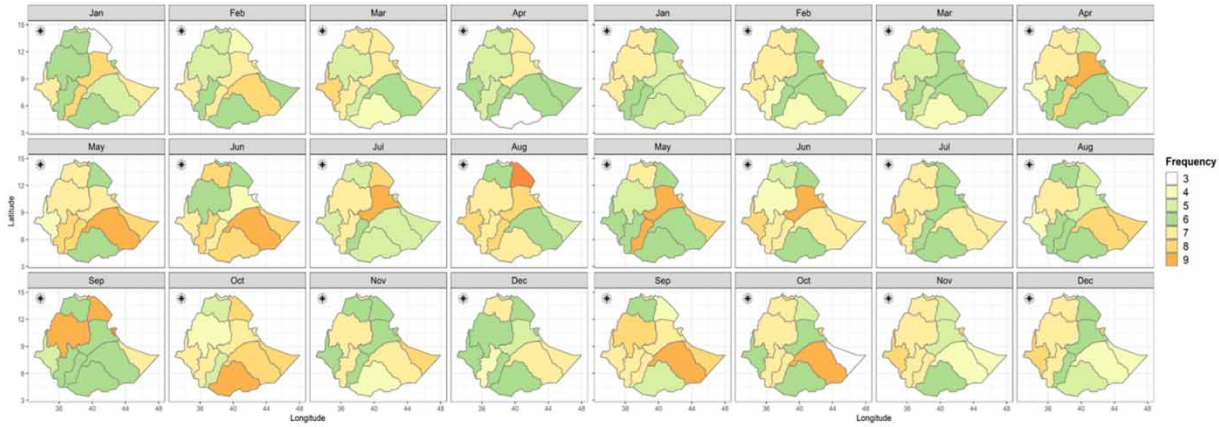

Figure 6 | Monthly drought episode frequency from monthly data using SPEI3 (a) and SPEI12 (b).

At a 12-month timescale, a hydrological drought event is more reflected (Figure 6(b)). Surprisingly, the monthly drought episode frequency did not show significant variations from that of SPEI3. It is slightly noticeable that drought happens more often in the Awash, Abbay, and Wabi-Shebele basins. Drought analysis studies in the country revealed that extreme hydrological drought occurs in the upper and middle Awash basin (Edossa *et al.* 2010) and the UBN basin (Bayissa *et al.* 2018).

Trend analysis

To better characterize the occurrence, characteristics and evolution of droughts in Ethiopia, the SPI and SPEI were calculated for the 12 major river basins that make up the country, which are represented in Figure 1. The time series of SPEI12 and SPI12, together with the trend of each series for each river basin of Ethiopia, is plotted in Figure 7. Except for a few instances, the peaks and troughs of each of the time series match closely and follow the same pattern and trend.

The highest and lowest values of SPI12 and SPEI12 provide a synopsis of hydrological dry and wet years. Major hydrological drought episode frequencies are identified in 1982, 2001, and 2011 with the most extended hydrological drought episode frequency occurring in the 1980s and early 2005 (El Kenawy *et al.* 2016). SPI and SPEI values from all the basins were, in general, highly correlated, specifying that either of the indices is suitable for drought depiction. The trends of SPEI12 and SPI12 for the Abbay, Aysha, Baro, Genale, Omo, Rift Valley, and Tekeze showed a positive trend. However, Wabi-Shebelle showed a decreasing trend. The difference between the two indices indicates the role of temperature in moderating the dryness trend.

For each of the 12 main river basins of Ethiopia, the M–Ke trend test and the Sen slope estimator were applied to investigate the overall trend of SPEI and SPI values at 1-, 3-, 6-, and 12-month timescales during the period 1981–2018. The slope of SPEI and SPI at 1-, 3-, 6-, and 12-month timescales can be found in Figure 8. The results showed predominantly positive trends (statistically significant) of the SPEI and the SPI on 3-, 6-, and 12-month timescales for Abbay, Baro, Omo, and Rift Valley river basins, which suggests that they experienced a tendency to become wetter. The remaining river basins (Awash, Aysha, Mereb, Ogaden, and Wabi-Shebelle) on the SPEI (SPI) at 1- and 3-month timescales experienced a tendency to become drier as revealed by negative trends of SPEI. The SPEI1 and SPEI3 negative trends were not statistically significant at a 95% confidence level. For the trends obtained in SPEI12 and SPI12, the drying (negative trend) was observed for Awash, Mereb, and Wabi-Shebelle; however, the trend was statistically significant only for Wabi-Shebelle. A significant wet (positive) trend was obtained for Abbay, Baro, Danakil, Ogaden, Omo, Rift Valley, and Tekeze. It is interesting to note that the magnitude of the slope is augmented when SPEI and SPI are computed with more lagged months. For instance, for the Abbay basin, the SPEI values were 0.691×10^{-3} and 2.692×10^{-3} for the 3-month timescale. A similar increase in the magnitude of the slope is observed for the SPI index. We can conclude that the wetting and drying magnitude of the main river basins of Ethiopia is significantly higher when computed at longer timescales. A spatial differentiation of drought index trends is observed between the basins occupying the eastern and western half of Ethiopia, suggesting an evolution toward opposite hydro-climatic conditions and characterized by a longitudinal differentiation.

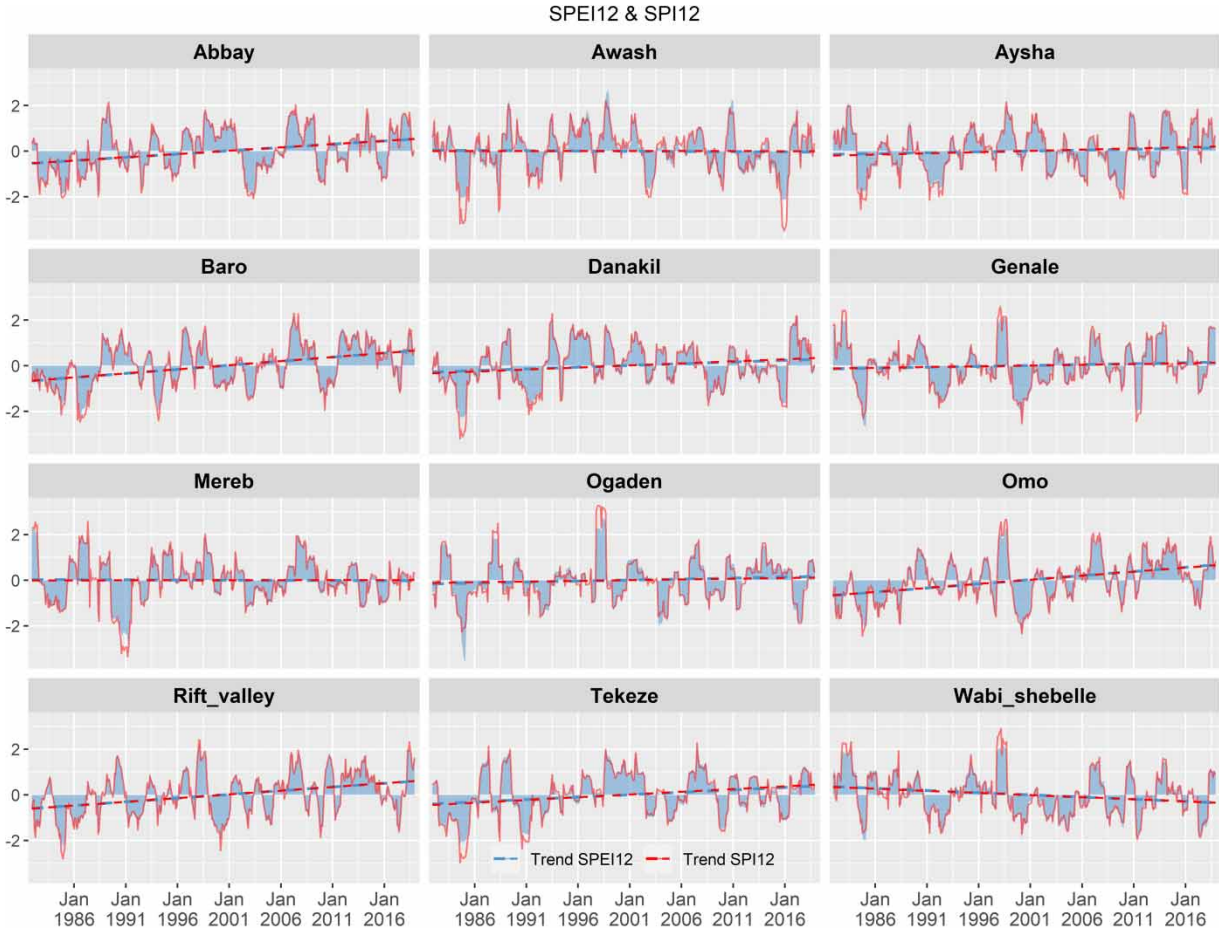

Figure 7 | Time series of SPEI12 (light blue) and SPI12 (red line) and their corresponding trend lines for the main river basins of Ethiopia during 1981–2018.

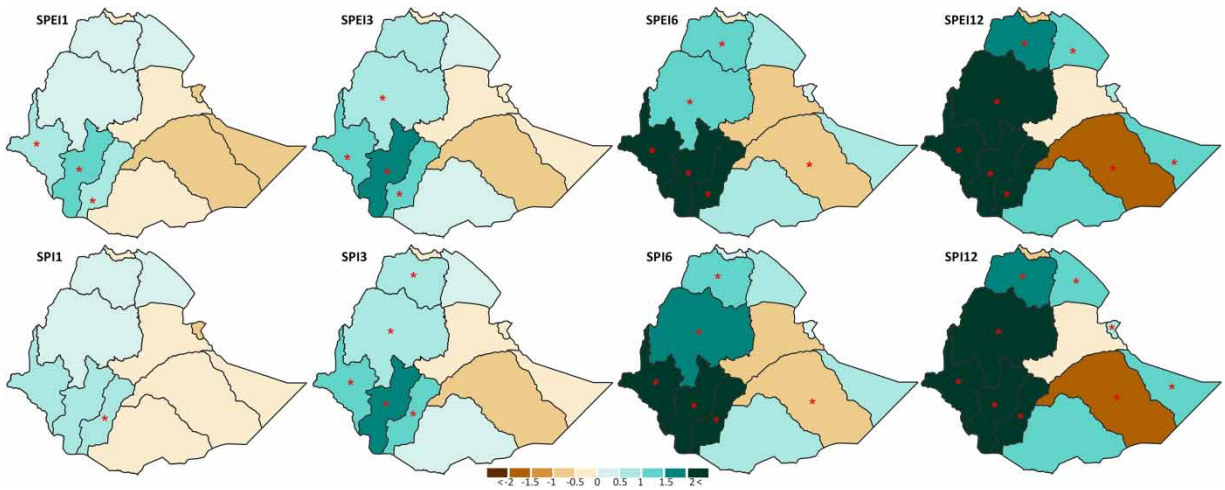

Figure 8 | The Sen's slope (×1,000) of the SPEI (top) and the SPI (bottom) at temporal scales of 1, 3, 6, and 12 months. Red asterisks indicate statistically significant trends at a 95% confidence level (period 1981–2018).

In Table 3, it is noted that differences among the SPEI and SPI trends were negative for the majority of the basins except for Baro, Omo, and Rift Valley for all analyzed timescales. For the analysis of drought conditions in the above basins, if we have only considered the SPI trend, we can only observe the wetting trend and favorable conditions. This is because the effect of temperature was omitted in the computation of SPI. A moderate trend than the SPI was identified by SPEI, which has considered the effect of temperature and thereby affecting the water balance of a region.

Teleconnections

Correlations between the gridded CHIRPS Ethiopian precipitation data at $0.05^\circ \times 0.05^\circ$ resolution and climate indices such as IOD, Nino 3.4, and PDO, which are well known to impact Ethiopian precipitation, are performed. The seasonal correlations map (only statistically significant values for $p < 0.05$) for the main rainfall seasons of March, April, May (MAM), June, July, August, September (JJAS), and October, November, December (OND) is presented in Figure 9. This figure shows the complex spatial variations of the seasonal teleconnections over Ethiopia. The MAM rainfall season, which is the primary precipitation season in southern Ethiopia, and the secondary rainfall season over central and northeastern Ethiopia are identified with a band of positive correlation with PDO extending from central Ethiopia to the northeast, while negative correlations are restricted over the Baro river basin in the west of the country. The correlation pattern with the IOD is highlighted because it is very similar but reversed in sign. Meanwhile, weak positive correlations with Nino 3.4 were found in the central region of the country. However, for JJAS, which is the primary precipitation season over most parts of Ethiopia, we found areas of negative correlations with Nino 3.4 to the center and northwest in the UBN and Tekeze, in agreement with previous findings (e.g. Diro *et al.* 2011; Degefu *et al.* 2017). In addition, areas with positive correlations are observed in the southeast over the Genale-Dawa, Wabi-Shebelle, and Ogaden. In JJAS, rainfall also displays a statistically significant positive relationship with IOD over the basins of the northeast of the country. Similarly, JJAS showed weak positive correlations with PDO but to the southeast. A correlation analysis for the OND season in southern Ethiopia (Kassahun 1987) displayed less teleconnection with all of the climate indices. So, it is rather striking that the OND shows a statistically significant positive correlation with the PDO in the south of the country, although the area that shows this relationship is visually small. In general, the correlation analysis between SST indices and gridded Ethiopian precipitation depicted in Figure 9 shows that SST fluctuations according to modes of climate variability in different forms for the seasonal and spatial pattern of precipitations over Ethiopia. Thus, for an enhanced and better-equipped forecasting of rains as well as other drought indicators, it is essential first to detect regional patterns and separate the country into uniform areas regarding the impacts of the SST.

Often the relationship between ENSO and droughts in Ethiopia, particularly during the El Niño phase, has been studied (Gebrekirstos *et al.* 2008; Zeleke *et al.* 2017; Gobie & Miheretu 2021). They found that droughts are significantly correlated with ENSO. One such common approach to analyzing ENSO teleconnections in the region is through composites of El Niño and La Niña. Though correlation can capture linear relationships, since it does not handle non-linear relationships,

Table 3 | The difference between SPEI (1, 3, 6, and 12) and SPI (1, 3, 6, and 12)

All basins	SPEI1 – SPI1	SPEI3 – SPI3	SPEI6 – SPI6	SPEI12 – SPI12
Abbay	−0.003	−0.046	−0.032	−0.012
Awash	**− 0.119**	**− 0.082**	**− 0.107**	**− 0.189**
Aysha	**− 0.3037**	**− 0.225**	**− 0.223**	**− 0.268**
Baro	0.005	0.010	0.085	0.049
Danakil	**− 0.109**	**− 0.143**	**− 0.209**	**− 0.1521**
Genale	−0.020	0.050	0.028	0.006
Mereb	**− 0.161**	0.005	0.031	**− 0.114**
Ogaden	**− 0.393**	−0.151	−0.013	0.044
Omo	0.015	0.017	**0.081**	**0.078**
Rift -Valley	0.006	0.021	**0.059**	0.012
Tekeze	**− 0.126**	−0.060	−0.013	**− 0.106**
Wabi-Shebelle	−0.064	−0.018	−0.052	**− 0.147**

The statistically significant trends at a 95% confidence level were represented with bold numbers.

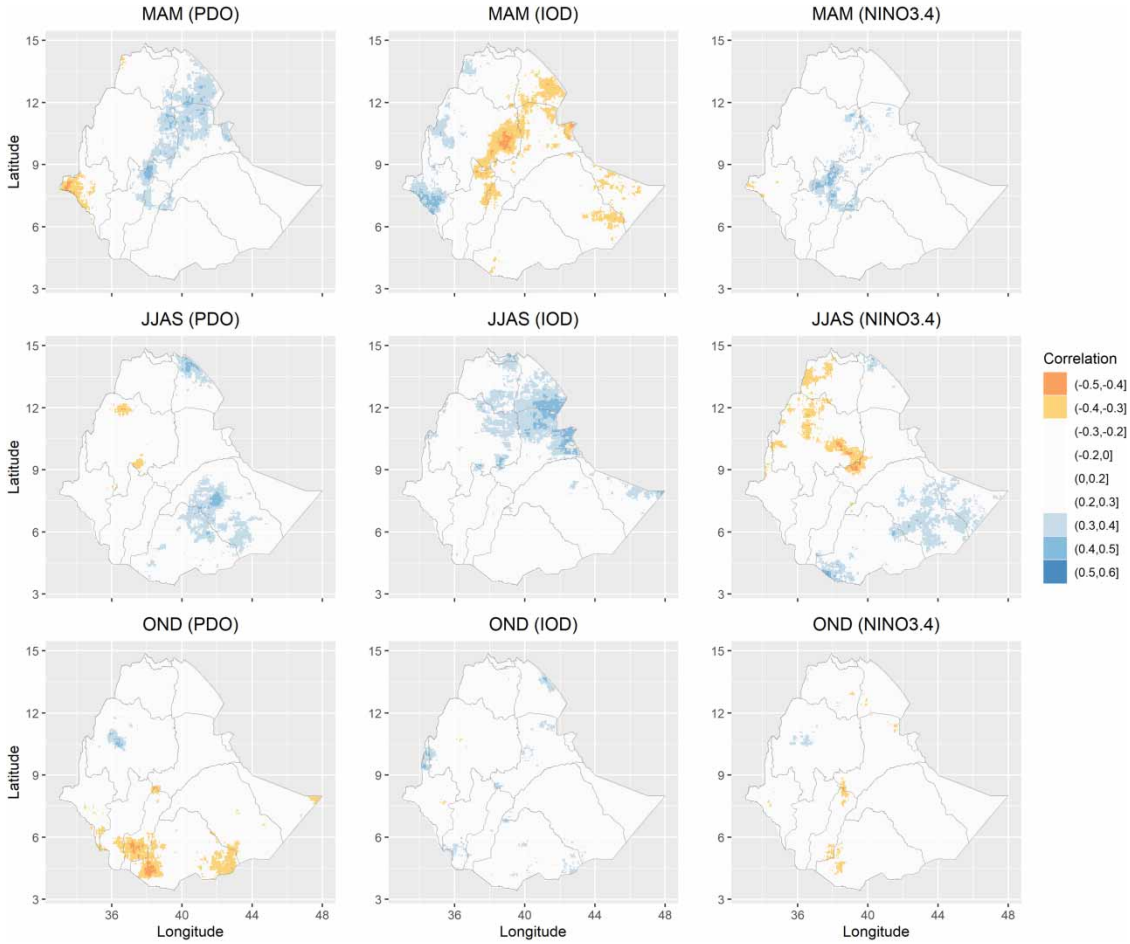

Figure 9 | Correlation between SST and seasonal precipitation over Ethiopia during 1981–2018. Both SST and precipitation data are averaged over the seasonal periods: MAM, JJAS, and OND.

composite analysis is widely used to understand physical mechanisms. There are various steps required to form composites of any given phenomenon. First is necessary to choose a means to define events for compositing. In a previous study on ENSO composite analysis, generally, a positive basis was utilized for El Niño events, and a negative basis was utilized for La Niña events (Karoly 1989). This study has used the definition of events described by the ONI to assign the events and nonevents. Especially, El Niño or La Niña events are compared with non-ENSO events. After the events are chosen, they are averaged. These averaged events are subtracted from the average of the nonevents to form the composite.

We can see from the composite maps (Figure 10) that the Ethiopian summer rainfall is influenced by SST over the eastern Pacific Ocean. When the eastern Pacific Ocean is anomalously warm (El Niño), large parts of the Ethiopian highlands get less rainfall. However, when the eastern Pacific Ocean is anomalously cold (La Niña), a small pocket region in the central and northern highlands areas of Ethiopia gets enhanced rainfall, whereas the southern region gets less rain.

Unlike other natural disasters, drought events evolve slowly in time, and large-scale atmospheric and oceanic teleconnections influence them. The effects of teleconnection in the river basins of Ethiopia are analyzed utilizing the Pearson correlation among climate indices and SPEI. In Figure 11, the Pearson correlation between the climate indices (DMI, ONI, PDO, and SOI) and SPEI in all the 12-month timescales for the period 1981–2018 is presented. This analysis allows us to determine the timescale by which the SPEI1–12 achieve the max correlation coefficient with the mode of climate variability. For the Abbay, Awash, Aysha, Danakil, and Tekeze basins, the best correlations were found for longer timescales of the SPEI. A significantly negative correlation was found with ONI, and a positive relationship was found with SOI. The results indicated that positive (negative) values of ONI are related with the occurrence of dry (wet) conditions in the basins. The analysis indicated that intense El Niño events were associated with dry conditions in the above basins, while the opposite

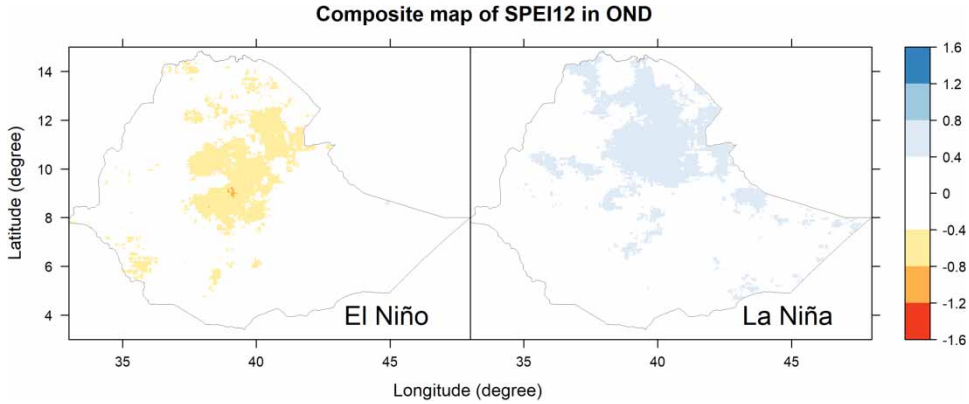

Figure 10 | Composite maps of precipitation in JJAS season during warm and cold ENSO years.

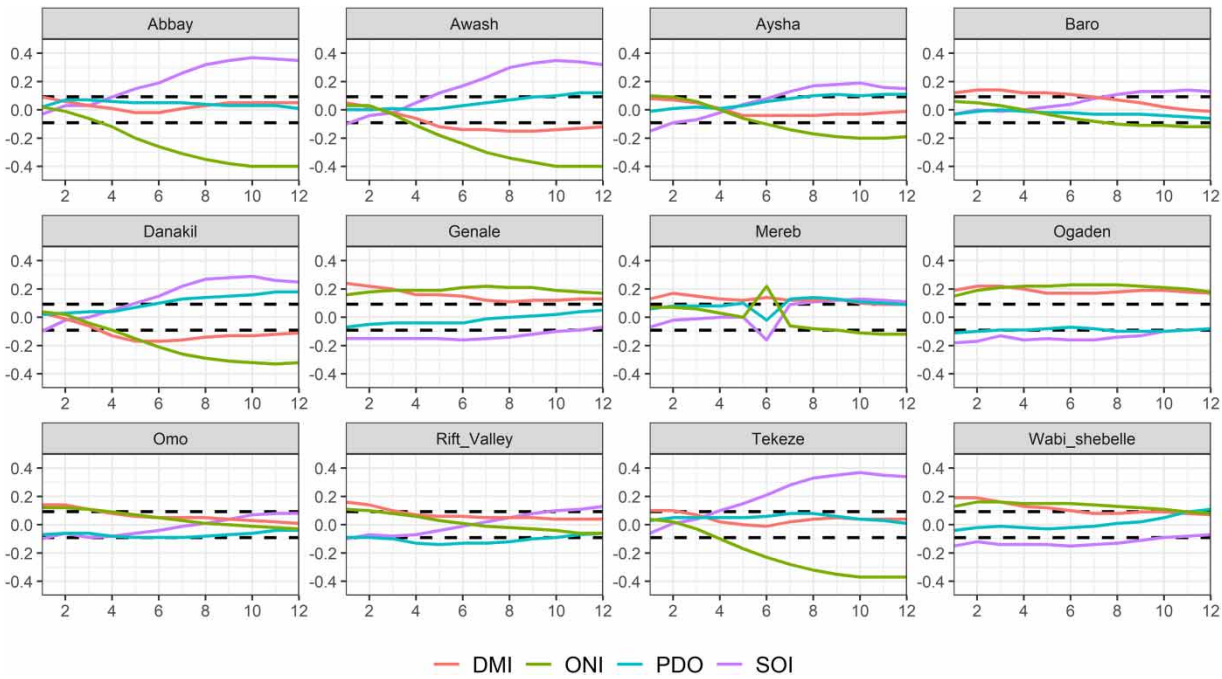

Figure 11 | Pearson correlation between DMI, ONI, PDO, SOI, and SPEI at 1–12 timescales. Black lines specify a statistically significant correlation coefficient at $p < 0.05$.

happened during La Niña. No significant correlation was found between PDO, DMI, and SPEI at longer timescales for the above basins; however, in Ogaden, Genale, there exists a weak significant correlation. Compared to the above basins, which mainly are located in the center, north, and northwest of the country, the correlations between Omo, Rift Valley, and Wabi-Shebelle situated in the south and southwest parts of Ethiopia showed some changes. For Baro and Omo, a statistically significant weak positive relationship between IOD and SPEI at shorter temporal scales was found. The SPEI is significantly higher during the warm phase of IOD, while low SPEI occurred during the negative phase of IOD. This specifies that the wet conditions in the southern region of Ethiopia are positively associated with the positive phase of IOD.

CONCLUSIONS

The primary aim of this research was to study and evaluate existing drought conditions and investigate their usefulness in assessing the impact of drought conditions on the environment of Ethiopia. The SPI and SPEI were applied to analyze drought

development over the study period. The analysis indicated that the main periods of drought occurred all over the country in 1982, 1984, 1987, 1991, 1997, 2002, 2006, 2011, and 2015. Similar temporal evolution of drought is observed from the SPI and SPEI series. However, the temporal drought analysis shows that there is a small difference in magnitude among the droughts depicted by the precipitation-based SPI and temperature-based SPEI as their difference (SPEI – SPI) was always negative, signifying the significant role of temperature and evapotranspiration processes on modulating the severity of drought.

Furthermore, this study assessed the role of various teleconnections on drought based on a composite analysis. Initially, we found different patterns of precipitation anomalies over Ethiopia associated with SST variations characterized through the ENSO index in the Atlantic Ocean, with the IDO index in the Indian Ocean, and with the Pacific Decadal Oscillation in the Pacific Ocean. The results highlight the relationship of El Niño with the occurrence of drought conditions in Ethiopia, highlighting its effect on cumulative drought conditions for timescales of more than 6–12 months. The precipitation anomalies for the JJAS period showed the impact of El Niño on the precipitation reduction in central highlands and favorable conditions during La Niña. This could be explained by the northeastward evolution of rainfall anomalies developing during El Niño. Interestingly, mild drought conditions are seen during MAM and OND with SPEI12. The effects of the La Niña event on drought conditions in Ethiopia are not clearly observed, as several areas in the northern, central, and eastern regions experienced abnormally wet conditions during La Niña events, especially in JJAS. The result showed that the rainfall over Ethiopia during the summer monsoon (JJAS) is negatively correlated with SST indices, and as such the study of the links between ENSO and drought occurrences, lagged correlations between ENSO and regional drought indicators such as rainfall can provide critical information for water resources and seasonal forecasts.

ACKNOWLEDGEMENTS

Milica Stojanovic acknowledges the grant no. ED481B-2021/134 from the Xunta of Galicia (regional government), and Rogert Sorí the grant RYC2021-034044-I funded by Ministerio de Ciencia, Innovación y Universidades, Spain (MICIU/AEI/10.13039/501100011033) and the European Union Next Generation EU/PRTR. Both are supported by the Xunta de Galicia under Project ED431C2021/44 (Programa de Consolidación e Estructuración de Unidades de Investigación Competitivas (Grupos de Referencia Competitiva) and the Consellería de Cultura, Educación e Universidade) and by the European Union `ERDF A way of making Europe'. This work has also been possible thanks to the computing resources and technical support provided by CESGA (Centro de Supercomputación de Galicia) and RES (Red Española de Supercomputación).

DATA AVAILABILITY STATEMENT

All relevant data are available from an online repository or repositories. The Nino sea surface temperature and PDO time-series values were obtained from the US National Center for Atmospheric Research (https://climatedataguide.ucar.edu/climate-data/nino-sst-indices-nino-12-3-34-4-oni-and-tni). The SOI values were acquired from the National Oceanic and Atmospheric Administration (https://www.ncdc.noaa.gov). The IOD index was obtained from the Japan Agency for Marine-Earth Science and Technology (https://www.jamstec.go.jp/frsgc/research/d1/iod/).

CONFLICT OF INTEREST

The authors declare there is no conflict.

REFERENCES

Abera, K., Gebeyehu, A., 2022 Review of hydrological drought analysis status in Ethiopia. In: *Drought – Impacts and Management* (Eyvaz, M., Albahnasawi, A., Tekbaş, M. & Gürbulak, E., eds). doi:10.5772/intechopen.102763ia.

Adnan, S., Ullah, K. & Gao, S. 2015 Characterization of drought and its assessment over Sindh, Pakistan during 1951–2010. *Journal of Meteorological Research* **29** (5), 837–857. https://doi.org/10.1007/S13351-015-4113-Z/METRICS.

Adnan, S., Ullah, K., Shuanglin, L., Gao, S., Khan, A. H. & Mahmood, R. 2018 Comparison of various drought indices to monitor drought status in Pakistan. *Climate Dynamics* **51** (5–6), 1885–1899. https://doi.org/10.1007/s00382-017-3987-0.

Ahmed, H., Tessema, Z. & Korecha, D. 2017 Inter-connection between El-Niño-Southern oscillation induced rainfall variability, livestock population dynamics and pastoralists adaptation strategies in Eastern Ethiopia. *Journal of Environment and Earth Science* **7** (3), 11–24.

Ahmed, J. S., Buizza, R., Dell' Acqua, M., Demissie, T. & Pè, E. 2024 Evaluation of ERA5 and CHIRPS rainfall estimates against observations across Ethiopia. *Meteorology and Atmospheric Physics* **136** (3). doi: 10.1007/s00703-024-01008-0.

AKLDP 2015 El Niño in Ethiopia uncertainties, impacts and decision-making. In: *Agriculture Knowledge, Learning Documentation and Policy (AKLDP) Project Ethiopia*. Feinstein International Center, Tufts University, Boston, MA. https://agri-learning-ethiopia.org/wp-content/uploads/2015/09/AKLDP-El-Nino-brief-Sept-2015.pdf

Allen, R. G., Pruitt, W. O., Wright, J. L., Howell, T. A., Ventura, F., Snyder, R., Itenfisu, D., Steduto, P., Berengena, J., Martin Smith, M., Pereira, L. S., Raes, D., Perrier, A., Alves, I., Walter, I. & Elliott, R. 2006 A recommendation on standardized surface resistance for hourly calculation of reference ETo by the FAO56 Penman-Monteith method. *Agricultural Water Management* **81**, 1–22. https://doi.org/10.1016/j.agwat.2005.03.007.

Almedeij, J. 2014 Drought analysis for Kuwait using Standardized Precipitation Index. *The Scientific World Journal* **2014**, 451841. https://doi.org/10.1155/2014/451841.

Ambelu, A. B. 2009 *Biological Monitoring Based on Macroinverteabrates for Decision Support of Water Management in Ethiopia.* Ghent University, Ghent.

Attia, B. B. & Abulhoda, A. B. 1992 The ENSO phenomenon and its impact on the Nile's hydrology. In: *Climate Fluctuations and Water Management* (Abu-Zeid, M.A. & Biswas, A.K., eds.). Butterworth Heinemann, Oxford, pp. 71–79.

Awulachew, S. B., Yilma, A. D., Loulseged, M., Loiskandl, W., Ayana, M. & Alamirew, T. 2007 *Water Resources and Irrigation Development in Ethiopia.* International Water Management Institute, Colombo, Sri Lanka. https://dlc.dlib.indiana.edu/dlcrest/api/core/bitstreams/0b62ab27-16dd-4b5a-a6cb-279f26f4abdd/content

Ayehu, G. T., Tadesse, T., Gessesse, B. & Dinku, T. 2018 Validation of new satellite rainfall products over the Upper Blue Nile Basin, Ethiopia. *Atmospheric Measurement Techniques* **11** (4), 1921–1936. https://doi.org/10.5194/AMT-11-1921-2018.

Babu, A. 2009 The impact of Pacific sea surface temperature on the Ethiopian rainfall'. Workshop on High Impact Weather Predictability Information Systemfor Africa and AMMA THORPEX Forecasters. Trieste, Italy: National Meteorological Agency. Available from: http://www.sciepub.com/reference/266543.

Bayissa, Y. A., Moges, S. A., Xuan, Y., Van Andel, S. J., Maskey, S., Solomatine, D. P., Van Griensven, A. & Tadesse, T. 2015 Spatio-temporal assessment of meteorological drought under the influence of varying record length: The case of Upper Blue Nile Basin, Ethiopia. *Hydrological Sciences Journal* **60** (11), 1927–1942. https://doi.org/10.1080/02626667.2015.1032291.

Bayissa, Y., Tadesse, T., Demisse, G. & Shiferaw, A. 2017 Evaluation of satellite-based rainfall estimates and application to monitor meteorological drought for the Upper Blue Nile Basin, Ethiopia. *Remote Sensing* **9** (7), 669. https://doi.org/10.3390/rs9070669

Bayissa, Y., Maskey, S., Tadesse, T., Van Andel, S. J., Moges, S., Van Griensven, A. & Solomatine, D. 2018 Comparison of the performance of six drought indices in characterizing historical drought for the upper Blue Nile Basin, Ethiopia. *Geosciences* **8** (3), 81.

Beguería, S., Vicente-Serrano, S. M. & Angulo-Martínez, M. 2010 A multiscalar global drought dataset: The SPEIbase: A new gridded product for the analysis of drought variability and impacts. *Bulletin of the American Meteorological Society* **91** (10), 1351–1354. https://doi.org/10.1175/2010BAMS2988.1.

Belay, A. S., Fenta, A. A., Yenehun, A., Nigate, F., Tilahun, S. A., Moges, M. M., Dessie, M., Adgo, E., Nyssen, J., Chen, M., Van Griensven, A. & Walraevens, K. 2019 Evaluation and application of multi-source satellite rainfall product CHIRPS to assess spatio-temporal rainfall variability on data-Sparse western margins of Ethiopian highlands. *Remote Sensing* **11** (22), 2688. https://doi.org/10.3390/RS11222688.

Bewket, W. & Conway, D. 2007 A note on the temporal and spatial variability of rainfall in the drought-prone Amhara region of Ethiopia. *International Journal of Climatology* **27** (11), 1467–1477. https://doi.org/10.1002/joc.1481.

Billi, P. 2015 Geomorphological landscapes of Ethiopia. In: *Landscapes and Landforms of Ethiopia* (Billi, P., ed.). Springer, Dordrecht,, pp. 3–32.

Camberlin, P. 1997 Rainfall anomalies in the source region of the Nile and their connection with the Indian summer monsoon. *Journal of Climate* **10** (6), 1380–1392. https://doi.org/10.1175/1520-0442(1997)010.

Comenetz, J. 2002 Climate variability, political crises, and historical population displacements in Ethiopia. Global Environmental Change Part B: Environmental Hazards. Available from: https://www.academia.edu/3665280/Climate_variability_political_crises_and_historical_population_displacements_in_Ethiopia.

Comenetz, J. & Caviedes, C. 2002 Climate variability, political crises, and historical population displacements in Ethiopia. *Global Environmental Change Part B: Environmental Hazards* **4** (4), 113–127. https://doi.org/10.3763/EHAZ.2002.0413.

CSA (Central Statistical Agency of Ethiopia) 2014 Agricultural Sample Survey. Report on Area and Production of Major Crops. Volume I, VII and VIII. Statistical Bulletin 578. CSA, Addis Ababa, Ethiopia.

Dai, A. 2013 Increasing drought under global warming in observations and models. *Nature Climate Change* **3** (1), 52–58. https://doi.org/10.1038/nclimate1633.

Degefu, M. A., Rowell, D. P. & Bewket, W. 2017 Teleconnections between Ethiopian rainfall variability and global SSTs: observations and methods for model evaluation. *Meteorology and Atmospheric Physics* **129**, 173–186.

Dinku, T., Ceccato, P., Grover-Kopec, E., Lemma, M., Connor, S. J. & Ropelewski, C. F. 2007 Validation of satellite rainfall products over East Africa's complex topography. *International Journal of Remote Sensing* **28** (7), 1503–1526. https://doi.org/10.1080/01431160600954688.

Diro, G. T., Toniazzo, T. & Shaffrey, L. 2011 Ethiopian rainfall in climate models. In: *African Climate and Climate Change. Advances in Global Change Research, vol 43* (Williams, C. & Kniveton, D., eds.). Springer, Dordrecht. https://doi.org/10.1007/978-90-481-3842-5_3.

Edossa, D. C., Babel, M. S. & Das Gupta, A. 2010 Drought analysis in the Awash River Basin, Ethiopia. *Water Resources Management* **24** (7), 1441–1460. https://doi.org/10.1007/S11269-009-9508-0/METRICS.

El Kenawy, A. M., McCabe, M. F., Vicente-Serrano, S. M., López-Moreno, J. I. & Robaa, S. M. 2016 Changes in the frequency and severity of hydrological droughts over Ethiopia from 1960 to 2013. *Cuadernos de Investigación Geográfica* **42** (1), 145–166. https://doi.org/10.18172/cig.2931.

Eltahir, E. A. B. 1996 El Niño and the natural variability in the flow of the Nile River. *Water Resources Research* **32** (1), 131–137.

Fenta, A. A., Yasuda, H., Shimizu, K., Ibaraki, Y., Haregeweyn, N., Kawai, T., Belay, A. S., Sultan, D. & Ebabu, K. 2018 Evaluation of satellite rainfall estimates over the Lake Tana basin at the source region of the Blue Nile River. *Atmospheric Research* **212**, 43–53. https://doi.org/10.1016/J.ATMOSRES.2018.05.009.

Funk, C., Peterson, P., Landsfeld, M., Pedreros, D., Verdin, J., Shukla, S., Husak, G., Rowland, J., Harrison, L., Hoell, A. & Michaelsen, J. 2015 The climate hazards infrared precipitation with stations – A new environmental record for monitoring extremes. *Scientific Data* **2**, 150066. https://doi.org/10.1038/sdata.2015.66.

Gebrehiwot, T., van der Veen, A. & Maathuis, B. 2011 Spatial and temporal assessment of drought in the Northern highlands of Ethiopia. *International Journal of Applied Earth Observation and Geoinformation* **13** (3), 309–321. https://doi.org/10.1016/J.JAG.2010.12.002.

Gebrekirstos, A., Mitlöhner, R., Teketay, D. & Worbes, M. 2008 Climate-growth relationships of the dominant tree species from semi-arid Savanna woodland in Ethiopia. *Trees – Structure and Function* **22** (5), 631–641. https://doi.org/10.1007/s00468-008-0221-z.

Gebremedhin, M. A., Lubczynski, M. W., Maathuis, B. H. P. & Teka, D. 2021 Novel approach to integrate daily satellite rainfall with in-situ rainfall, Upper Tekeze Basin, Ethiopia. *Atmospheric Research* **248**. https://doi.org/10.1016/j.atmosres.2020.105135.

Gidey, E., Dikinya, O., Sebego, R., Segosebe, E., Zenebe, A., Gidey, E., Dikinya, O., Sebego, R., Segosebe, E. & Zenebe, A. 2018 Modeling the spatio-temporal meteorological drought characteristics using the Standardized Precipitation Index (SPI) in Raya and its environs, Northern Ethiopia. *ESE* **2** (2), 57. https://doi.org/10.1007/S41748-018-0057-7.

Gobie, B. G. & Miheretu, B. A. 2021 Effects of El Nino southern oscillation events on rainfall variability over northeast Ethiopia. *Modeling Earth Systems and Environment* **7** (4), 2733–2739. https://doi.org/10.1007/s40808-020-01060-w.

Hargreaves, G. H. 1975 Moisture availability and crop production. *Transactions of the ASAE* **18** (5), 980–0984. https://doi.org/10.13031/2013.36722.

Hirpa, F. A., Gebremichael, M. & Hopson, T. 2010 Evaluation of high-resolution satellite precipitation products over very complex terrain in Ethiopia. *Journal of Applied Meteorology and Climatology* **49** (5), 1044–1051. https://doi.org/10.1175/2009JAMC2298.1.

IPCC 2021 Climate Change 2021: The Physical Science Basis. In *Contribution of Working Group I to the Sixth Assessment Report of the Intergovernmental Panel on Climate Change* (Masson-Delmotte, V., Zhai, P., Pirani, A., Connors, S.L., Péan, C., Berger, S., Caud, N., Chen, Y., Goldfarb, L., Gomis, M.I., Huang, M., Leitzell, K., Lonnoy, E., Matthews, J.B.R., Maycock, T.K., Waterfield, T., Yelekçi, O., Yu, R. & Zhou, B., eds.). Cambridge University Press, Cambridge, UK and New York, NY.

Jain, V. K., Pandey, R. P., Jain, M. K. & Byun, H. R. 2015 Comparison of drought indices for appraisal of drought characteristics in the Ken River Basin. *Weather and Climate Extremes* **8**, 1–11. https://doi.org/10.1016/J.WACE.2015.05.002.

Kaniewski, D., Van Campo, E. & Weiss, H. 2012 Drought is a recurring challenge in the Middle East. *Proceedings of the National Academy of Sciences of the United States of America* **109** (10), 3862–3867. https://doi.org/10.1073/PNAS.1116304109/SUPPL_FILE/PNAS.201116304SI.PDF.

Karoly, D. J. 1989 Southern hemisphere circulation features associated with El Niño-Southern Oscillation events. *Journal of Climate* **2** (11), 1239–1252.

Kassahun, B. 1987 Weather systems over Ethiopia. In *Proc. First Tech. Conf. on Meteorological Research in Eastern and Southern Africa*, Nairobi, Kenya, UCAR, pp. 53–57.

Koo, J., Thurlow, J., ElDidi, H., Ringler, C. & De Pinto, A. 2019 Building resilience to climate shocks in Ethiopia. *Food Policy Reports*. Available from: https://ideas.repec.org/p/fpr/fprepo/9780896293595.html.

Kourouma, J. M., Eze, E., Kelem, G., Negash, E., Phiri, D., Vinya, R., Girma, A. & Zenebe, A. 2022 Spatiotemporal climate variability and meteorological drought characterization in Ethiopia. *Geomatics, Natural Hazards and Risk* **13** (1), 2049–2085. https://doi.org/10.1080/19475705.2022.2106159

Kumar, B. G. 2008 Ethiopian famines 1973–1985: A case-study. In: *The Political Economy of Hunger: Volume 2: Famine Prevention*, pp. 173–216. https://doi.org/10.1093/acprof:oso/9780198286363.003.0004.

Lehner, B., Henrichs, T., Döll, P. & Alcamo, J. 2001 Eurowasser model-based assessment of European water resources and hydrology in the face of global change. *Kassel World Water Series* **5** (December), 1–6. Available from: https://pure.au.dk/portal/en/publications/eurowasser–modelbased-assessment-of-european-water-resources-and-hydrology-in-the-face-of-global-change(450019f0-7e9e-11dd-a5a8-000ea68e967b)/export.html.

Lemma, E., Upadhyaya, S. & Ramsankaran, R. 2022 Meteorological drought monitoring across the main river basins of Ethiopia using satellite rainfall product. *Environ Syst Res* **11**, 7. https://doi.org/10.1186/s40068-022-00251-x.

Li, Y., Huang, S., Wang, H., Zheng, X., Huang, Q., Deng, M. & Peng, J. 2021 High-resolution propagation time from meteorological to agricultural drought at multiple levels and spatiotemporal scales. *Agricultural Water Management* **262**, 107428. https://doi.org/10.1016/j.agwat.2021.107428.

McKee, T. B., Doesken, N. J. & Kleist, J. 1993 The relationship of drought frequency and duration to time scales. In *Proceedings of the Eighth Conference on Applied Climatology*, Anaheim, CA, 17–22 January 1993, pp. 179–184. https://www.droughtmanagement.info/literature/AMS_Relationship_Drought_Frequency_Duration_Time_Scales_1993.pdf

Mann, H. B. 1945 Non-parametric test against trend. *Econometrika* **13**, 245–259.

Mersha, A. A. & van Laerhoven, F. 2018 The interplay between planned and autonomous adaptation in response to climate change: Insights from rural Ethiopia. *World Development* **107**, 87–97. https://doi.org/10.1016/j.worlddev.2018.03.001.

Molla, F., Kebede, A. & Raju, U. J. P. 2019 The impact of the El-Niño southern oscillation precipitation and the surface temperature over the Upper Blue Nile Region. *Journal of Scientific Research and Reports* **21** (5), 1–15. https://doi.org/10.9734/JSRR/2018/45657.

Mondol, M. A. H., Das, S. C. & Islam, M. N. 2016 Application of Standardized Precipitation Index to assess meteorological drought in Bangladesh. *Jàmbá: Journal of Disaster Risk Studies* **8** (1), 1–14. https://doi.org/10.4102/JAMBA.V8I1.280.

Mukherjee, S., Mishra, A. & Trenberth, K. E. 2018 Climate change and drought: A perspective on drought indices. *Current Climate Change Reports* **4** (2), 145–163. https://doi.org/10.1007/S40641-018-0098-X.

Mulualem, G. M. & Liou, Y. A. 2020 Application of artificial neural networks in forecasting a standardized precipitation evapotranspiration index for the Upper Blue Nile Basin. *Water* **12** (3), 643. https://doi.org/10.3390/W12030643.

Naumann, G., Cammalleri, C., Mentaschi, L. & Feyen, L. 2021 Increased economic drought impacts in Europe with anthropogenic warming. Nature Climate Change **11**, 485–49. https://doi.org/10.1038/s41558-021-01044-3

Park, J. H., Kim, K. B. & Chang, H. Y. 2014 Statistical properties of effective drought index (EDI) for Seoul, Busan, Daegu, Mokpo in South Korea. *APJAS* **50** (4), 453–458. https://doi.org/10.1007/S13143-014-0035-4.

Ravazzani, G., Corbari, C., Morella, S., Gianoli, P. & Mancini, M. 2012 Modified Hargreaves-Samani equation for the assessment of reference evapotranspiration in Alpine river basins. *Journal of Irrigation and Drainage Engineering* **138** (7), 592–599.

Roop, S., Mulugeta, W., Bogale, S., Cullis, A., Adem, A., Irwin, B., Lim, S., Bosi, L. & Venton, C. C. 2016 Reality of resilience: Perspectives of the 2015–16 drought in Ethiopia. *BRACED – Resilience Intel* **6**, 28.

Saji, N. H., Goswami, B. N., Vinayachandran, P. N. & Yamagata, T. 1999 A dipole mode in the tropical Indian ocean. *Nature* **401** (6751), 360–363. https://doi.org/10.1038/43854.

Salvador, S., Nieto, R., Vicente-Serrano, S., Garcia-Herrera, R., Gimeno, L. & Vicedo-Cabrera, A. M. 2023 Public health implications of drought in a climate change context: a critical review. *Annual Review of Public Health* **44**, 213–232. https://doi.org/10.1146/annurev-publhealth-071421-051636.

Silva, J. A. & Uchida, R. 2000 Agriculture and Food Security | Nepal | U.S. Agency for International Development. In 2000. Available from: https://www.usaid.gov/ethiopia/agriculture-and-food-security.

Stojanovic, M., Mulualem, G. M., Sorí, R., Vázquez, M., Nieto, R. & Gimeno, L. 2022 Precipitation moisture sources of Ethiopian river basins and their role during drought conditions. *Frontiers in Earth Science* **10**, 929497.

Suryabhagavan, K. V. 2017 GIS-based climate variability and drought characterization in Ethiopia over three decades. *Weather and Climate Extremes* **15**, 11–23. https://doi.org/10.1016/J.WACE.2016.11.005.

Tallaksen, L. M. & Van Lanen, H. A. J. 2004 Hydrological drought: Processes and estimation methods for streamflow and groundwater. *Development in Water Science* **48**, 579.

Thornthwaite, C. W. 1948 An approach toward a rational classification of climate. *Geographical Review* **38** (1), 55. https://doi.org/10.2307/210739.

Tigkas, D., Vangelis, H. & Tsakiris, G. 2015 Drinc: A software for drought analysis based on drought indices. *Earth Science Informatics* **8** (3), 697–709. https://doi.org/10.1007/s12145-014-0178-y.

Trisos, C. H., Adelekan, I. O., Totin, E., Ayanlade, A., Efitre, J., Gemeda, A., Kalaba, K., Lennard, C., Masao, C., Mgaya, Y., Ngaruiya, G., Olago, D., Simpson, N. P. & Zakieldeen, S. 2022 Chapter 9: Africa. In: *Climate Change 2022: Impacts, Adaptation and Vulnerability. Contribution of Working Group II to the Sixth Assessment Report of the Intergovernmental Panel on Climate Change* (Pörtner, H.-O., Roberts, D.C., Tignor, M., Poloczanska, E.S., Mintenbeck, K., Alegría, A., Craig, M., Langsdorf, S., Löschke, S., Möller, V., Okem, A. & Rama, B., eds.). Cambridge University Press, Cambridge and New York, NY, pp. 1285–1455.

Tsakiris, G., Pangalou, D. & Vangelis, H. 2007 Regional drought assessment based on the Reconnaissance Drought Index (RDI). *Water Resources Management* **21** (5), 821–833. https://doi.org/10.1007/S11269-006-9105-4/METRICS.

Vicente-Serrano, S. M., Beguería, S. & López-Moreno, J. I. 2010 A multiscalar drought index sensitive to global warming: the standardized precipitation evapotranspiration index. *Journal of Climate* **23** (7), 1696–1718. https://doi.org/10.1175/2009JCLI2909.1.

Viste, E., Korecha, D. & Sorteberg, A. 2013 Recent Drought and Precipitation Tendencies in Ethiopia. *Theoretical and Applied Climatology* **112**, 535–551.

WMO 2012 Standardized Precipitation Index User Guide. World Meteorological Organization, Geneva, Switzerland. https://www.droughtmanagement.info/literature/WMO_standardized_precipitation_index_user_guide_en_2012.pdf

Wolde-Georgis, T. 1997 El Niño and drought early warning in Ethiopia. *Internet Journal of African Studies* **2** (2), 10.

Yu, C., Li, C., Xin, Q., Chen, H., Zhang, J., Zhang, F., Li, X., Clinton, N., Huang, X., Yue, Y. & Gong, P. 2014 Dynamic assessment of the impact of drought on agricultural yield and scale-dependent return periods over large geographic regions. *Environmental Modelling & Software* **62**, 454–464. https://doi.org/10.1016/J.ENVSOFT.2014.08.004.

Zargar, A., Sadiq, R., Naser, B. & Khan, F. I. 2011 A review of drought indices. *Environmental Reviews* **19** (1), 333–349. https://doi.org/10.1139/A11-013.

Zeleke, T., Giorgi, F. & Mengistu Tsidu, G. 2013 Spatial and temporal variability of summer rainfall over Ethiopia from observations and a regional climate model experiment. *Theoretical and Applied Climatology* **111**, 665–681. https://doi.org/10.1007/s00704-012-0700-4.

Zeleke, T. T., Giorgi, F., Diro, G. T. & Zaitchik, B. F. 2017 Trend and periodicity of drought over Ethiopia. *International Journal of Climatology* **37** (13), 4733–4748. https://doi.org/10.1002/joc.5122.

Zeleza, P. T. & McCann, J. C. 1997 People of the plow: An agricultural history of Ethiopia, 1800–1990. *Technology and Culture* **38** (4), 980. https://doi.org/10.2307/3106971.

Zhong, R., Chen, X., Lai, C., Wang, Z., Lian, Y., Yu, H. & Wu, X. 2019 Drought monitoring utility of satellite-based precipitation products across Mainland China. *Journal of Hydrology* **568**, 343–359. https://doi.org/10.1016/J.JHYDROL.2018.10.072.

Zinna, A. W. & Suryabhagavan, K. V. 2016 Remote sensing and GIS based spectro-agrometeorological maize yield forecast model for South Tigray Zone, Ethiopia. *Journal of Geographic Information System* **08** (02), 282–292. https://doi.org/10.4236/JGIS.2016.82024.

First received 26 December 2023; accepted in revised form 4 May 2024. Available online 15 May 2024